



Published in final edited form as:

J Biomed Mater Res A. 2014 May ; 102(5): 1467–1477. doi:10.1002/jbm.a.34821.

A Biodegradable Thermoset Polymer Made by Esterification of Citric Acid and Glycerol

Jeffrey M. Halpern¹, Richard Urbanski², Allison K. Weinstock², David F. Iwig³, Robert T. Mathers², and Horst von Recum¹

¹Department of Biomedical Engineering, Case Western Reserve University, Cleveland, OH 44106

²Department of Chemistry, Pennsylvania State University, New Kensington, PA 15068

³Alcoa Technical Center, 100 Technical Drive, Alcoa Center, PA 15069

Abstract

A new biomaterial, a degradable thermoset polymer, was made from simple, economical, biocompatible monomers without the need for a catalyst. Glycerol and citric acid, non-toxic and renewable reagents, were crosslinked by a melt polymerization reaction at temperatures from 90-150°C. Consistent with a condensation reaction, water was determined to be the primary byproduct. The amount of crosslinking was controlled by the reaction conditions, including temperature, reaction time, and ratio between glycerol and citric acid. Also, the amount of crosslinking was inversely proportional to the rate of degradation. As a proof-of-principle for drug delivery applications, gentamicin, an antibiotic, was incorporated into the polymer with preliminary evaluations of antimicrobial activity. The polymers incorporating gentamicin had significantly better bacteria clearing of *Staphylococcus aureus* compared to non-gentamicin gels for up to nine days.

1 Introduction

The use of crosslinking in polymers, effectively generating thermoset materials, has received widespread attention as a means to tailor device properties for use in vascular and osseous tissue.¹⁻⁴ The improved mechanical performance of crosslinked biomaterials aids as a scaffold for cell growth, as well as varying degrees of controlled drug release, or biodegradability.^{2,5,6}

Biodegradable polymers in biomedical applications are frequently made with ester bonds, due to their capacity for hydrolytic cleavage, although other linkages based on carbonyl derivatives, such as imines, amides, and anhydrides, have also been reported.⁶⁻¹⁰ Such clinically used polyesters are typically thermoplastic polymers, such as poly(lactic acid) (PLA), poly(ϵ -caprolactone), and poly(*L*-lactic-*co*-glycolic acid) (PLGA).^{11,12} In contrast to thermoset polymers, thermoplastic polymers are less mechanically robust, which limits the ability to tailor them for a broad range of applications.

Various biodegradable polymers, made from either citric acid or glycerol, have previously been researched with mixed results. Biodegradable ester materials based on glycerol were made with various carboxylates (*e.g.* sebacate), fabricated at a high temperature under a low-pressure argon environment.¹³⁻¹⁵ For example, glycerol and sebacic acid were reacted without a catalyst to form poly-glycerol sebacate (PGS), which shows promising biocompatibility and biodegradability results.¹⁵ However, due to the high hydrophobicity of sebacic acid, degradation and biological fate of the monomers and short oligomers are often complicated by solubility issues. The local release of sebacic acid leads to a higher concern about local pH change than would occur upon release of hydrophilic citric acid. Further,

citric acid, as used herein, is more readily available and of lower cost than sebacic acid. In regards to polymers based on citric acid, other papers have described reacting citric acid with polyethylene glycol to create thermoplastic tri-block dendrimer macro- and nano-molecules for drug delivery systems; however, these polymers showed limited biodegradability.¹⁶⁻¹⁹ Also the thermoplastic materials would have minimal branching, and therefore only modest mechanical property change, as compared to the high crosslinking potential of the described thermoset materials. Finally, citric acid was previously reacted with glycerol in solution and in the presence of benzene and p-toluenesulfonic acid (PTSA) to form a crosslinked ester copolymer.²⁰ Although this resulting citric acid and glycerol polyester showed promise as a drug delivery system, the incorporation of carcinogens, such as benzene and PTSA, created compatibility complications for biomedical and pharmaceutical applications.

Our research group has explored the synthesis of a new crosslinked, thermoset polymer, which can be made with a wide range of degradation and mechanical parameters and is made from simple, economical, bio-available reagents without the need for a catalyst. In addition, the chemistry is non-complex and can be conducted in air, at atmospheric pressure. Our goal was to design a polymer with the following properties: a) uses ester bonds to take advantage of hydrolytic cleavage; b) is only made from low cost, non-toxic renewable components; c) retains the capacity to control the rate of degradation; and d) has the capability of incorporating chemical functionalities, deliverable drugs, and nutrients. For the first two properties, the use of non-toxic, pharmaceutical grade, ester bond-forming components, we identified citric acid and glycerol (listed as one of top 12 renewable chemicals by the U.S. Department of Energy)²¹ as non-toxic renewable resources and biologically safe nutrients, being generally regarded as safe (GRAS) by the U.S. Food and Drug Administration.^{4,22,23} Both have been identified as building blocks for a platform to deliver pharmaceuticals.^{16-20,24,25} For the third desired property, the rate of degradation has been found to be inversely proportional to the amount of crosslinking, and it is possible to vary the amount of crosslinking of citric acid and glycerol. Lastly, chemical functionality or deliverable payload (e.g. antibiotics) can be integrated into this crosslinked system during fabrication to create an effective delivery mechanism.

This article describes the esterification of citric acid and glycerol using a condensation reaction mechanism to fabricate a new thermoset polymer capable of drug delivery. Initial studies used conventional catalysts; however, we observed a high yield even without the use of catalysts. Varying the amount of glycerol was a convenient method to control the physical properties, degree of crosslinking, and biodegradability. Additionally, the melt polymerization only produced water as a by-product of the condensation reaction. In proof-of-principle studies, gentamicin was incorporated into the polymer to serve as a model drug, as its presence can be easily evaluated by its antibacterial properties. While ongoing work is underway in our labs to evaluate drug loading following polymer synthesis, or to synthesize the polymer under lower temperatures, the current materials require drugs which are stable at moderately high temperatures. Since gentamicin is well-known to show minimal to no degradation at temperatures below 121°C,²⁶ is served an excellent model drug for incorporation and delivery in the current system.

2 Experimental Section

2.1 Materials

Glycerol (99%, Sigma-Aldrich), *para*-toluenesulfonic acid monohydrate (PTSA) (97.5%, Acros Organics), zinc (II) chloride (97+%, Acros Organics), and gentamicin (BioReagent, Sigma-Aldrich) were used as received. Citric acid (anhydrous, 99.5%, Acros) was ground into powder with mortar and pestle and filtered through a brass sieve (150 μm, Fisher

Scientific). Aluminum pans (7cm diameter, Fisher Scientific) and buffer solution pH 7.40 (certified pH 7.39-7.41 @25° C, Fisher Scientific) were used as received.

2.2 General Method for Polymerization of Glycerol and Citric Acid

Freshly ground anhydrous citric acid powder (8.0 mmol) was sieved through a 150 μm brass sieve into a 7.0 cm aluminum pan with glycerol (8.0 mmol). One experimental control dish was set up with no catalyst added. The two other dishes also contained PTSA (0.08 mmol, 1 mol %) and ZnCl_2 (0.08 mmol, 1 mol %). The three dishes were placed in oven set at a set temperature and time before being removed and allowed to cool to ambient temperature.

Subsequent trials of polymerization methods include the increase of the glycerol to citric acid ratio from 1:1 to 2:1 and 3:1, as well as other variations specified within the text.

For the gentamicin incorporated experiments, 1.6:1 ([glycerol]:[citric acid]) and 5 mol% gentamicin was polymerized at 110°C for three different reaction times--7, 15, and 48 hrs-- to create low crosslinked, medium crosslinked, and high crosslinked polymers, respectively. 5 mol% gentamicin was chosen because it successfully dissolved in glycerol, and also, this concentration lead towards effective antibacterial activity, however further optimization is possible.

2.3 Polymer Characterization

The decomposition temperature (T_d) was determined with a TA Instruments thermo-gravimetric analysis (TGA) Q500 at 20° C/min under a flow of nitrogen (30 mL/min). Polymer samples (4-8 mg) were placed on platinum pans and heated from 30-650° C. The reported decomposition temperature (T_d) values were calculated from the onset of decomposition using the peak from the first derivative of the weight loss to identify the maximum slope.

Mechanical analysis was measured with a TA Instruments Q800 dynamic mechanical analyzer (DMA). A five point temperature calibration was performed. The reaction of glycerol and citric acid ([gly]/[CA] = 1) was examined at a frequency of 1 Hz and amplitude of 30 μm . The sample bar (35 mm \times 13 mm \times 1.7 mm), which was backed with aluminum foil, was removed from a Teflon mold after curing for 2 hours and placed in a single cantilever clamp. The modulus was measured at 110° C.

FTIR spectra (32 scans) were recorded with a ZnSe ATR crystal at a 4 cm^{-1} resolution on a ThermoFisher Nicolet iS10 FTIR spectrometer.

2.4 Kinetic evaluation of Glycerol and Citric Acid

Reaction kinetics were evaluated by measuring the water lost in relation to the percentage of hydroxyl groups reacted. Three separate trials of 1:1 ratio glycerol to citric acid were set up, and each was run in a gas chromatography (GC) oven at separate temperatures of 90°C, 110°C, and 130°C for a minimum of ten hours each. Samples were removed from the oven at intervals and weighed. The weights were recorded and calculated for weight loss to determine the formation of ester groups. Given the large boiling point differences between glycerol (bpt 290° C) and water at atmospheric pressure, all mass loss was attributed to water formation. The % OH groups that reacted were calculated with the formula: (g of water lost) \times (1/18.015 g mol^{-1}) \times (1/maximum mol water) \times 100. The maximum mol of water that could be theoretically produced by esterification reactions was: (g citric acid/ 192.12 g mol^{-1}) \times 3. The kinetic profiles were obtained by graphing the resulting % OH values as a function of time.

2.5 Liquid Chromatography Mass Spectroscopy (LC/MS) Characterization

High performance liquid chromatography (HPLC)-grade water was added to a resin sample and was thoroughly mixed. After 1 hour, a 1 μ L aliquot was injected into a Waters Acquity UPLC in line with a Thermo Scientific LTQ-Orbitrap in ESI(+) mode. The UPLC system was equipped with a BEH phenyl column (130 \AA , 1.7 μ m, 2.1 mm \times 75 mm) equilibrated in 95% solvent A (0.1% formic acid) and 5% solvent B (0.1% formic acid in acetonitrile) at 0.400 mL/min. Mass spectra data were collected using full Fourier transform mode with 30000 resolution. The compounds containing gentamicin eluted between 0.40 and 0.60 minutes; the mass spectra across all peaks in this time period were averaged, and the neutral mass spectrum was extracted using the associated Thermo Scientific Qual Browser 2.0.7 SP1 software.

2.6 Bacteria-Clearing Assays

Antimicrobial activity was examined using both a dynamic, solution-based bacterial clearing assay and a static zone of inhibition study. The high agitation of the solution-based assay tends to more effectively model mixing, solvent action, and removal of degradation products than a static assay. The zone of inhibition assay tends to have higher sensitivity and to better model the low vascularity and diffusional exchange present in the environments in which many of these materials are used (e.g. subcutaneous, intraosseous), compared to a dynamic, solution-based assay. While neither are accurate predictors of biological performance, both have been previously used to describe new materials and delivery systems and to indicate that the release is application dependent.²⁷⁻³² Similarly, the ASTM E2149 – 10 Standard Test Method calls for both solution testing and zone of inhibition assays.³³

For the solution-based bacterial assay 30 g BBL Trypticase Soy Broth (Becton, Dickinson Company) was dissolved in 1 L Milli-Q water and autoclaved at 121°C for 20 min. Bacteria were freshly grown by placing frozen *Staphylococcus aureus* (*S. aureus* kindly provided by Dr. Edward Greenfield, Case Western Reserve University) into a 15ml Falcon tube prepared with 5 mL sterile soy broth and incubated for overnight at 37°C on an orbital shaker (~225 rpm).

105-140g of high, medium, and low crosslinking polymer were each placed into a 15ml - Falcon tube with 5 mL soy broth. Two controls were prepared, (1) a tube with control polymer not loaded with drug, and (2) a tube with no polymer present, with the latter used to normalize the measurements. Each tube was infected with 10 μ L freshly grown bacteria and incubated for 20-24 hrs on a 37°C orbital shaker. The *S. aureus* solution was completely removed and replaced with fresh *S. aureus* solution each day for a period of six days. All tubes were done in triplicate.

Each sample was prepared in three dilutions to ensure at least one measurement was in the linear range of the calibration. The calibration curve was generated by producing a dilution series from the sample with no polymer. The samples were read at two absorbance wavelengths, 485 nm and 595 nm, and the determined % clearing was averaged, assuming that the control tubes with no polymer had 100% bacteria.

For the static, zone of inhibition assay, also known as the Kirby-Bauer Assay, plates were prepared as previously described.³⁴ As mechanical breakdown and sample fragmentation occurred during the course of the study, it was challenging to continue to transfer entire samples from plate to plate which is required for a conventional Kirby-Bauer Assay. To circumvent this, samples were placed into a porous tissue culture insert with 1 μ m pore size, and the assay run by moving this insert from plate to plate. This ensured that released drug could escape to have antimicrobial effect, but that as the sample fragmented all fragments

larger than $1\mu\text{m}$ were contained together. We had previously validated this procedure using other work in our lab (manuscript under review). In this study, specifically 32 mg of medium and high crosslinked polymer were placed in Transwell porous tissue culture inserts (6 cm) (N=3). Before the zone of inhibition assay, the samples were soaked for 1.5 hrs in a 200 μL phosphate buffered saline (PBS) solution. The water was removed by Kimwipe underneath the Transwell. In addition, 20 μL of PBS solution was added after every transfer to aid in media transfer between polymer and bacteria-infected soy broth agar. The zones were measured and the Transwell plates were transferred to new bacteria plates every day.

3 Results

3.1 Polymer Formation and Characterization

The reaction of an alcohol with a carboxylic acid is a well-studied reaction that forms an ester under non-catalytic or catalytic conditions.³⁵ Common catalysts include Bronsted acids, Lewis acids, enzymes, and solid acids. As demonstrated by TGA data in Figure 1, the melt polymerization of glycerol and citric acid with catalysts PTSA and ZnCl_2 generates a polyester network with greater thermal stability compared to the onset of weight loss for citric acid (197°C) and glycerol (209°C). In addition, characterization of a sample bar by dynamic mechanical analysis (DMA) indicated an increase in the storage modulus (Figure 2) as a function of time. The large increase in the storage modulus indicated that the reaction of glycerol and citric acid produced a crosslinked network with robust physical properties. DMA also detected glass transition temperatures (T_g) based on the maximum of the $\tan \delta$ peak, which represents the ratio of storage to loss moduli. After heating the film at 110°C , the T_g increased to 61°C after 24 hr, and the T_g increased to 83°C after 48 hr. These data demonstrate the generation of a crosslinked network between citric acid and glycerol.

In the absence of a catalyst, the equilibrium could be shifted towards the products by the removal of water, either by increasing the temperature or by decreasing the pressure. As depicted in Scheme 1, the reaction between glycerol and citric acid proceeded at temperatures above 90°C . Using FTIR spectroscopy, the ester formation was accompanied by a decrease in the OH (3290 cm^{-1}) and C-O (1032 cm^{-1}) absorbances for glycerol. In Figure 3, the initial C=O absorbance for citric acid (1694 cm^{-1}) was gradually replaced by ester absorbances at 1724 cm^{-1} (C=O stretch) and 1176 cm^{-1} (C-O).

In order to determine the optimum ratio of [glycerol]/[citric acid] for fabricating a polymer useable in drug delivery, several ratios were characterized by TGA (Figure 4). The two-stage decomposition profile of the TGA curves indicates that the crosslinking between glycerol and citric acid depends on the molar ratio of [glycerol]:[citric acid]. The samples with a 1:1 glycerol to citric acid ratio had 30% decomposition at 300°C compared to the samples with 2:1 and 3:1 ratios, which had 60% decomposition. This comparison indicates that the optimum ratio of [glycerol]:[citric acid] for biomedical applications will be expected to fall between 1:1 and 2:1.

In addition to controlling the degree of crosslinking with the ratio of [glycerol]/[citric acid], the influence of time on the polyester thermoset was also investigated. In Figure 5, samples with a 1:1 ratio of glycerol to citric acid were prepared and reacted at 150°C for 0.5 hr, 1.0 hr, and 3.0 hr. All three samples in this experiment showed two different stages of weight loss that was previously seen in Figure 1. As time was increased, an increase in the amount of ester formation was observed. After a 3.0 hr reaction time, a higher percentage of polymer remained at 325°C with a concomitant decrease in the initial decomposition of the sample. Since it was observed that the reactivity at 150°C proceeded very quickly, even after 0.5 hr without a catalyst, lower temperatures were examined to investigate the optimal method for the synthesis of a drug delivery system.

3.2 Kinetic Data of Crosslinked Reaction

In Figure 6, the kinetic data from the reaction of glycerol and citric acid was examined by measuring the percent of OH groups reacted as a function of time. Since this reaction undergoes Fischer esterification, producing water as a by-product, the percent of OH groups reacted was calculated by measuring the proportional amount of water loss. The boiling points of glycerol (290°C) and the decomposition temperature of citric acid (175°C) ensure that water is the only compound being driven off, with decarboxylation not suspected as a source of weight loss in the absence of PTSA and temperatures below 150°C.

In each of the three trials, reacted at different temperatures 90°C, 110°C, and 130°C, the reacted OH groups follow a logarithmic profile, with R^2 equal to 0.908, 0.989, and 0.998 respectively (Figure 4, top). After 12 hrs, the number of OH groups ranges between 54%-85% (90°C-130°C), indicating a high level of control over the variability in the amount of crosslinking within the polymer.

The initial number of reacted OH groups (up to 3.5 hrs) exhibited a linear profile of R^2 values of 0.999, 0.989, and 0.926 for the curing temperatures of 90°C, 110°C, and 130°C respectively (Figure 4, bottom). The number of OH groups for the first 3.5 hrs ranged between 27%-65% (90°C-130°C), indicating a greater level of control yet less crosslinking as compared to the longer time plot. The 90°C curing temperature provided the greatest amount of linear control in the OH groups reacted, but the 130°C curing temperature provided the greatest amount of crosslinking.

3.3 Polymer Formation with Gentamicin

Gentamicin was added to the melt polymerization to incorporate a therapeutic agent into the polymer. Our hypothesis was that while some gentamicin would remain unreacted and free for delivery, some gentamicin would directly crosslink within the citric acid-glycerol polymer, potentially changing the crosslinking groups of the polymer. The polymer with gentamicin was tinted orange; the polymer without gentamicin was clear. The control polymer with a 1:1 ratio ([glycerol]:[citric acid]) was reacted for 66 hrs at 110°C. Figure 7 confirms that gentamicin loaded into the melt before polymerization leads to crosslinking changes, resulting in a lower initial degradation temperature as a result of gentamicin-citric acid or gentamicin-glycerol oligomers. The second degradation was greater in the polymers crosslinked with gentamicin, indicating that the gentamicin-loaded polymers had a greater crosslinking density of ester bonds with potential amine bonds.

The gentamicin oligomers were confirmed using LC/MS. A polymer sample with gentamicin was submersed in water and sampled. Figure 6 confirms that gentamicin forms oligomers with both citric acid and glycerol. The cartoons above the mass spectrum peaks represent the number of monomers bound to the gentamicin but do not indicate a particular sequence distribution.

The mass spectra for each gentamicin-containing compound yielded three multiple $M+$ peaks: the expected value at a given m/z , a peak at -14.016 corresponding to the absence of a methylene unit ($-\text{CH}_2$) on gentamicin, and a peak at -28.032 corresponding to the absence of an ethylene unit ($-\text{C}_2\text{H}_4$) (or two methylene units) on gentamicin. Investigation into where the methylene groups (or ethylene group) were located was not performed; however, the resulting peak cluster pattern was used to identify gentamicin-containing peaks in the mass spectra. Additionally, m/z values corresponding to one or two water losses (18.011 g/mol and 36.022 respectively) were observed for each compound and were also used to identify the gentamicin-containing compounds. Efforts to discover the exact locations of the

covalent linkages were not made; therefore, no specific regiochemistry or order of linkages is implied in Figure 8.

The following m/z values were observed in the averaged mass spectrum: 477.3149 (gentamicin, expected 477.3163, -2.83 ppm error); 633.3203 (gentamicin-citrate, one water loss, expected 633.3221, -2.89 ppm error); 707.3569 (gentamicin-citrate-glycerol, one water loss, expected 707.3589, -2.84 ppm error); 863.3615 (gentamicin-dicitrate-glycerol, two water losses, expected 863.3648, -3.81 ppm error); 937.3982 (gentamicin-dicitrate-diglycerol, two water losses, expected 937.4016, -3.60 ppm error); 1015.4298 (demethylgentamicin-dicitratetriglycerol, one water loss, expected 1015.4330, -3.41 ppm error); and 1097.3975 (demethylgentamicin-tricitrate-diglycerol, two water losses, expected 1097.4024, -4.43 ppm error).

3.4 Anti-Bacterial Activity

Polymers loaded with gentamicin were used to clear cultures of *Staphylococcus aureus* (*S. aureus*), in both solution assays and zone of inhibition studies, to demonstrate activity after formulation as compared to polymers without gentamicin, Figures 9 and 10. As described in Figure 7, three separate polymers loaded with gentamicin were reacted for 7, 15, and 48 hrs to fabricate low, medium, and high crosslinked polymers.

Bacterial solution clearing from all polymers, including the non-gentamicin control, was observed for the first two days, but clearing in later days was only seen with drug loaded polymers (Figure 9). We hypothesized that the initial clearing was caused by the release of unbound citric acid, which resulted in a pH change of the soy broth, and that bacteriacidal activity was initially due to this pH change. The pH of polymers undergoing similar degradation in a phosphate buffer saline solution showed a rapid decrease to pH 2.9-3.2 in the initial solution in which these were placed. The pH would likely be even lower in the non-buffered soy broth at the first time point.

Due to completely changing the release media every day, bacterial clearing at subsequent time points was believed to be caused only by gentamicin release. This was confirmed by statistically significant differences of bacteria clearing in gentamicin samples as compared to the non-gentamicin control, after day 2. For low crosslinking density polymers with gentamicin, significant clearing was observed on Day 2 ($p < 0.05$) and Day 3 ($p < 0.005$) compared to the control (no gentamicin) polymer. Medium crosslinking density polymers with gentamicin had significant clearing only on Day 3 ($p < 0.005$) compared to the control. Finally, the high crosslinking polymer with gentamicin had significant clearing later, on Days 3 & 4 ($p < 0.005$) compared to the control.

The low crosslinked polymers degraded rapidly with little intact polymer by 3 days, and the medium crosslinked polymers showed noticeable degradation by day 6. In both cases, no significant bacteria clearing was observed after substantial polymer degradation, indicating the majority of drug was released. The high crosslinked polymers with gentamicin remained intact even up to 6 days, presumably with free and chemically bound gentamicin still within (based on LCMS data).

Medium and high crosslinked polymers were further tested over a period of 10 days using a zone of inhibition assay (Figure 10). Medium crosslinked polymers showed a zone of inhibition until the polymer showed noticeable degradation around day 4. High crosslinked polymers showed a consistently smaller zone of inhibition than medium crosslinked polymers but did not show signs of degradation until after 9 days. The profiles observed in the Kirby Bauer Assay are typical of a diffusion-based release profile.^{36,37} With the lower crosslinked polymers, the more rapid burst observed is most likely due to smaller oligomers

breaking up, resulting in a local decrease in diffusivity and allowing a quick release of unbound gentamicin.

4 Discussion

The crosslinking of glycerol and citric acid was examined as a biodegradable material. The influences of polymerization time, temperature, and catalyst on the physical properties of the polymer were examined.

Experiments were conducted to determine if the reaction would benefit from the use of a catalyst. Figure 1 shows that PTSA does improve the thermal stability but is not necessary to produce a reaction. While PTSA improves thermal stability of the reaction at lower reaction temperatures, it reduces the stability of citric acid at higher reaction temperatures due to decarboxylation. In early experiments, decarboxylation was visually confirmed by the formation of bubbles and a decrease in the carbonyl absorbance in the FTIR. Consequently, further experiments were pursued without a catalyst.

Although a reaction of citric acid and glycerol in the melt is more challenging without a catalyst, it is beneficial from both a green chemistry standpoint and a biocompatibility perspective since unnecessary additives are eliminated. From the standpoint of biodegradation, a catalyst-free reaction eliminates concerns related to leaching unwanted products (*e.g.* stannous catalysts used in PLGA formulation). The greater acidity of citric acid ($pK_a = 3.13$)³⁸ compared to other carboxylic acids, such as benzoic acid ($pK_a = 4.25$),³⁹ sebacic acid ($pK_a = 4.72$)⁴⁰, and acetic acid ($pK_a = 4.75$),³⁹ is believed to better catalyze the esterification process.

The crosslinking between glycerol and citric acid resulted in a two-stage decomposition profile compared to citric acid alone. According to the TGA data, ester groups that formed during the glycerol and citric acid reaction resulted in an increased degradation temperature compared to citric acid. This was confirmed with FTIR data, Figure 3. As the ester conversion increased, crosslinking increased the thermal stability. The 1:1 molar ratio [glycerol]/[citric acid] is stoichiometrically favorable to creating a larger crosslinked fraction as compared to an increased molar ratio. The two-stage profile in Figure 4 resulted from the presence of smaller oligomers, or side chains, which decompose at lower temperatures (190°C) than the crosslinked fraction (300-325°C) at an increased molar ratio [glycerol: citric acid].

The polymerization reaction between citric acid and glycerol without a catalyst was investigated as a function of time. As determined by TGA, Figure 5 illustrates that decomposition at lower temperatures decreases as the reaction progresses, indicating the presence of fewer small oligomers. Similarly, decomposition at higher temperatures increases as the reaction progresses, which indicates the presence of a larger crosslinked fraction. The progression of the reaction is confirmed by Figure 6, which also suggests the ability to control the % of crosslinking occurring within the reaction.

Proof-of-principle drug loading and delivery results using gentamicin as a model drug were presented. Gentamicin is well-known for its use in preventing or treating device infection, specifically orthopaedic implant infection.⁴¹ Local delivery of antibiotics to combat orthopaedic implant infections is a growing field; however, many existing thermoplastic materials are unsuited to this purpose.⁴²

Three different degrees of crosslinking were presented in Figures 7-10: low crosslinking (7 hr polymerization reaction), medium crosslinking (15 hr polymerization reaction), and high crosslinking (48 hr polymerization reaction). As expected, the low crosslinked polymer

degraded the fastest in the soy broth solution-based bacteria clearing assay. By degrading the quickest, it released all of the incorporated gentamicin within the first three days, resulting in greater bacteria clearing, (Figure 9, $p < 0.005$) but for a shorter time. The medium crosslinked polymer degraded in 6 days in a solution based assay. Over that time, days 4-6, the bacteria clearing trended less than the control (Figure 9), indicating some release of gentamicin into the media over that time period. The release of gentamicin in an aqueous environment was confirmed by LC/MS, as shown in Figure 8. It is likely that this reduced antibiotic activity is due to the formation of gentamicin oligomers with citric acid and/or glycerol. Finally, the high crosslinked polymer did not degrade much in the 6 days in which the bacterial solution clearing was performed, but it did clear bacteria significantly in early time points (days 3-4). The bacteria clearing caused by medium and high crosslinked polymers were confirmed by zone of inhibition assay, Figure 10. Both polymers showed good clearing in the first four days, and the high crosslinked gentamicin loaded polymers showed good clearing for up to 9 days.

The shelf-life of the polymer in a desiccator at room temperature was qualitatively evaluated over 1.5 years. The bacteria clearing assay was conducted both immediately after fabrication (data not shown) and up to 6 months later with similar results (Figure 9). The Kirby-Bauer Assay data was conducted 1.5 years after formulation, demonstrating antibacterial activity even after longer-term storage. At the time of the Kirby-Bauer Assay, the low crosslinked polymer had begun to soften, which was presumably due to some degradation. More crosslinked polymers showed no visual indications of degradation even after 1.5 years of dry storage, yet some minor unobserved degradation may have occurred. Because of the ester bond, we do not expect a long shelf-life in humid, heated conditions.

Based on qualitative bench-top tests, we have found the polymer has over a 1.5 year shelf-life in a desiccator stored at room temperature. The bacteria clearing assay was conducted both immediately after fabrication and up to 6 months later with similar results (data not shown). The Kirby-Bauer Assay data was conducted 1.5 yrs after formulation, demonstrating antibacterial activity even after longer-term storage. At the time of the Kirby-Bauer Assay, the low crosslinked polymer had begun to soften. This was presumably due to some degradation and may have also occurred in the more crosslinked formulations, yet the more crosslinked polymers showed no visual indications of degradation even after 1.5 years of dry storage. Because of the ester bond, we do not expect a long shelf-life in humid, heated conditions.

Based on the LC/MS data, Figure 8, the amine groups on gentamicin are able to react with the ester groups to form amide bonds. As a result, it appears that the greater crosslinking density benefits the physical durability of the polymers at the expense of a quick release of gentamicin. Although a fraction of the gentamicin was temporarily sequestered by the formation of amide bonds, the ubiquitous presence of enzymes such as amidases in biological systems would be expected to hydrolyze these amide bonds to free gentamicin.⁴³ Also it is possible that various oligomers of gentamicin themselves have antibacterial activity.

5 Conclusion

We have demonstrated that the reaction between citric acid and glycerol occurs without a catalyst and that the only predicted byproduct of the reaction is water, which is removed during the reaction with heat. Varying degrees of crosslinking were observed by changing various reaction conditions: time, temperature, and molar ratios. The final product was an estercrosslinked biodegradable polymer. Integration of gentamicin into the polymer melt allowed for the incorporation and release of a therapeutic agent. Statistically significant

bacteria clearing of *S. aureus* was shown to change with the degree of crosslinking in polymers loaded with gentamicin. In future work, other temperature-insensitive therapeutic agents will be integrated into the polymer melt, or other agents can be loaded through other means (e.g. solvent loading) for delivery in a biodegradable fashion.

Acknowledgments

This investigation was supported in part by the National Institutes of Health Ruth L. Kirschstein National Research Service Award T32 AR007505 (JMH). RTM thanks the Alcoa Foundation for support of green chemistry and sustainability at Penn State.

References

1. Bettinger, C.J.; Borenstein, J.T.; Langer, R. Micro- and nanofabricated scaffolds.. In: Lanza, R.; Langer, R.; Vacanti, J., editors. *Principles of Tissue Engineering*. Elsevier Academic Press; Burlington: 2007. p. 341-358.
2. Scholz M-S, Blanchfield JP, Bloom LD, Coburn BH, Elkington M, Fuller JD, Gilbert ME, Muflahi SA, Pernice MF, Rae SI. The use of composite materials in modern orthopaedic medicine and prosthetic devices: A review. *Composites Science and Technology*. 2011; 71:1791–1803. others.
3. Chung EJ, Kodali P, Laskin W, Koh JL, Ameer GA. Long-term *in vivo* response citric acid-based nanocomposites for orthopaedic tissue engineering. *J. Mater Sci. Mater Med*. 2011; 22:2131–2138. [PubMed: 21786133]
4. Witowski J, Knapowski J. Glycerol toxicity for human peritoneal mesothelial cells in culture: comparison with glucose. *Int. J. Artif. Organs*. 1994; 17(5):252–260. [PubMed: 7960193]
5. Pachence, J.M.; Bohrer, M.P.; Kohn, J. Biodegradable polymers.. In: Lanza, R.; Langer, R.; Vacanti, J., editors. *Principles of Tissue Engineering*. Elsevier Academic Press; Burlington: 2007. p. 323-340.
6. Holland TA, Mikos AG. Review: Biodegradable Polymeric Scaffolds. Improvements in Bone Tissue Engineering through Controlled Drug Delivery. *Adv. Biochem. Engin./Biotechnol*. 2006; 102:161–185.
7. Engineer C, Parikh J, Raval A. Review on Hydrolytic Degradation Behavior of Biodegradable Polymers from Controlled Drug Delivery Systems. *Trends in Biomater. Artif. Organs*. 2011; 25(2)
8. Rezwan K, Chen QZ, Blaker JJ, Boccaccini AR. Biodegradable and bioactive porous polymer/inorganic composite scaffolds for bone tissue engineering. *Biomaterials*. 2006; 27(18):3413–3431. [PubMed: 16504284]
9. Nam HY, Nam K, Hahn HJ, Kim BH, Lim HJ, Kim HJ, Choi JS, Park J-S. Biodegradable PAMAM ester for enhanced transfection efficiency with low cytotoxicity. *Biomaterials*. 2009; 30:665–673. [PubMed: 18996585]
10. Wiskur SL, Lavigne JJ, Metzger A, Tobey SL, Lynch V, Anslyn EV. Thermodynamic analysis of receptors based on guanidinium/boronic acid groups for the complexation of carboxylates, α -hydroxylcarboxylates, and diols: Driving force for binding and cooperativity. *Chem. Eur. J*. 2004; 10:3792–3804. [PubMed: 15281164]
11. Mathers, R.T.; Meier, M.A., editors. *Green Polymerization Methods: Renewable Starting Materials, Catalysis and Waste Reduction*. Wiley-VCH; Weinheim: 2011.
12. Doi, Y.; Steinbuchel, A., editors. *Biopolymers. Polyesters III. Applications and Commercial Products*. Wiley-VCH; Weinheim: 2002.
13. Bettinger CJ, Orrick B, Misra A, Langer R, Borenstein JT. Microfabrication of poly (glycerolsebacate) for contact guidance applications. *Biomaterials*. 2006; 27:2558–2565. [PubMed: 16386300]
14. Wang Y, Ameer GA, Sheppard BJ, Langer R. A tough biodegradable elastomer. *Nature Biotechnology*. 2002; 20:602–606.
15. Wang Y, Kim YM, Langer R. *in vivo* degradation characteristics of poly(glycerol sebacate). *J. Biomed Mater Res*. 2003; 66A:192–197.

16. Namazi H, Adeli M. Dendrimers of citric acid and poly (ethylene glycol) as the new drug-delivery agents. *Biomaterials*. 2005; 26:1175–1183. [PubMed: 15451637]
17. Namazi H, Adeli M, Zarnegar Z, Dadkhah A, Shukla A. Encapsulation of nanoparticles using linear-dendritic macromolecules. *Colloid Polym. Sci*. 2007; 285:1527–1533.
18. Namazi H, Jafarirad S. Investigation on some physicochemical properties of guest-conjugated and -incorporated hybrid organic/inorganic linear-dendritic nanocarriers. *J. Polym. Res*. 2011; 18:1431–1440.
19. Naeini AT, Adeli M, Vossoughi M. Poly(citric acid)-block-poly(ethylene glycol) copolymers - new biocompatibility hybrid materials for nanomedicine. *Nanomedicine: Nanotechnology, Biology, and Medicine*. 2010; 6:556–562.
20. Parmanick D, Ray TT. Synthesis and biodegradation of copolyesters from citric acid and glycerol. *Polymer Bulletin*. 1988; 19(4):365–370.
21. Manzer, LE. Biomass derivatives: A sustainable source of chemicals.. In: Bozell, JJ.; Patel, MK., editors. *Feedstocks for the Future: Renewables for the Production of Chemicals and Materials*. American Chemical Society; Washington, DC: 2006.
22. de Sousa SMG, Bramante CM, Taga EM. Biocompatibility of EDTA, EGTA, and Citric Acid. *Braz. Dent. J*. 2005; 16(1):3–8. [PubMed: 16113926]
23. Porter, WL. Recent Trends in Food Applications of Antioxidants.. In: Simic, M.; Karel, G., editors. *Autoxidation in Food and Biological Systems*. Plenum Press; New York: 1980. p. 295-365.
24. Zhang X, Tang H, Hoshi R, De Laporte L, Qui H, Xu X, Shea LD, Ameer GA. Sustained transgene expression via citric acid-based polyester elastomers. *Biomaterials*. 2009; 30:2632–2641. [PubMed: 19200593]
25. Yang J, Webb AR, Ameer GA. Novel citric acid-based biodegradable elastomers for tissue engineering. *Advanced Materials*. 2004; 16:511–516.
26. Traub WH, Leonhard B. Heat stability of the antimicrobial activity of sixty-two antibacterial agents. *Journal of Antimicrobial Chemotherapy*. 1995; 35:149–154. [PubMed: 7768762]
27. Silici S, Koc AN. Comparative study of in vitro methods to analyse the antifungal activity of propolis against yeasts isolated from patients with superficial mycoses. *Lett Appl Microbiol*. 2006; 43:318–324. [PubMed: 16910939]
28. Yin HQ, Langford R, Burrell RE. Comparative evaluation of the antimicrobial activity of ACTICOAT antimicrobial barrier dressing. *J. Burn Care Rehabil*. 1999; 20:195–200. [PubMed: 10342470]
29. Lee D, Cohen RE, Rubner MF. Antibacterial properties of Ag nanoparticle loaded multilayers and formation of magnetically directed antibacterial microparticles. *Langmuir*. 2005; 21:9651–9659. [PubMed: 16207049]
30. Anand A, Pundir R, Pandian CS, Saraf S, Gupta H. Cefoperazone sodium impregnated polycaprolactone composite implant for osteomyelitis. *Indian J. Pharm. Sci*. 2009; 71:377–381. [PubMed: 20502542]
31. Bhatta RS, Chandasana H, Chhonker YS, Rathi C, Kumar D, Mitra K, Shukla PK. Mucoadhesive nanoparticles for prolonged ocular delivery of natamycin: In vitro and pharmacokinetics studies. *Int. J. Pharm*. 2012; 432:105–112. [PubMed: 22569234]
32. Guarda A, Rubilar JF, Miltz J, Galotto MJ. The antimicrobial activity of microencapsulated thymol and carvacrol. *Int. J. Food Microbiol*. 2011; 146:144–150. [PubMed: 21411168]
33. International, A. Standard Test Method for Determining the Antibacterial Activity of Immobilized Antimicrobial Agents Under Dynamic Contact Conditions. Volume ASTM Standard E2149-10. ASTM International; West Conshohocken, PA: 2010.
34. Thatiparti TR, Shoffstall AJ, von Recum HA. Cyclodextrin-based device coating for affinity-based release of antibiotics. *Biomaterials*. 2010; 31:2335–2347. [PubMed: 20022369]
35. Otera, J.; Nishikido, J. *Esterification: Methods, Reactions, and Applications*. Wiley; Weinheim: 2010.
36. Halpern JM, von Recum HA, Ma P. *Affinity-based Drug Delivery Systems*. Biomaterials and Regenerative Medicine. 2013
37. Wang NX, von Recum HA. Affinity-based drug delivery. *Macromolecular Bioscience*. 2011; 11:321–332. [PubMed: 21108454]

38. Haynes, WM., editor. CRC Handbook of Chemistry and Physics. 91st ed.. CRC Press; Boca Raton: 2010. Dissociation Constants of Organic Acids and Bases.; p. 8-46.
39. Bordwell FG. Equilibrium acidities in dimethyl sulfoxide solution. *Acc. Chem. Res.* 1988; 21:456–463.
40. Bretti C, Crea F, Foti C, Sammartano S. Solubility and activity coefficients of acidic and basic nonelectrolytes in aqueous salt solutions. 2. Solubility and activity coefficients of suberic, azelaic, and sebacic acids in NaCl(aq), (CH₃)₄NCl(aq), and (C₂H₅)₄NI(aq) at different ionic strengths and at t = 25°C. *J. Chem. Eng. Data.* 2006; 51:1660–1667.
41. Lee D-W, Yun Y-P, Park K, Kim SE. Gentamicin and bone morphogenic protein-2 (BMP-2)-delivering heparinized-titanium implant with enhanced antibacterial activity and osteointegration. *Bone.* 2012; 50:974–982. [PubMed: 22289658]
42. Campoccia D, Montanaro L, Speziale P, Arciola CR. Antibiotic-loaded biomaterials and the risks for spread of antibiotic resistance following their prophylactic and therapeutic clinical use. *Biomaterials.* 2010; 31:6363–6377. [PubMed: 20542556]
43. Sharma M, Sharma NN, Bhalla TC. Amidases: Versatile enzymes in nature. *Rev. Environ. Sci. Biotechnol.* 2009; 8:343–366.

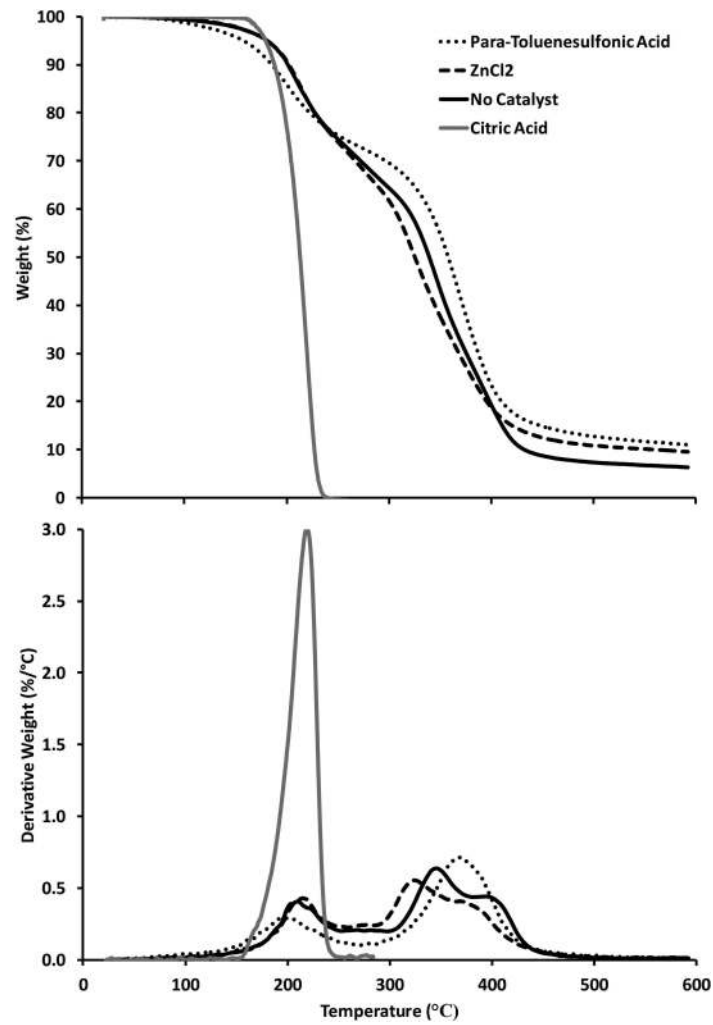


Figure 1. TGA data (20°C/min) for the reaction of glycerol and citric acid at 110°C using 1 mol% paratoluenesulfonic acid, 1 mol% ZnCl₂, and no catalyst. TGA data for unreacted citric acid is shown for comparison. Top: Weight percent as a function of temperature. Bottom: Derivative of weight percent as a function of temperature.

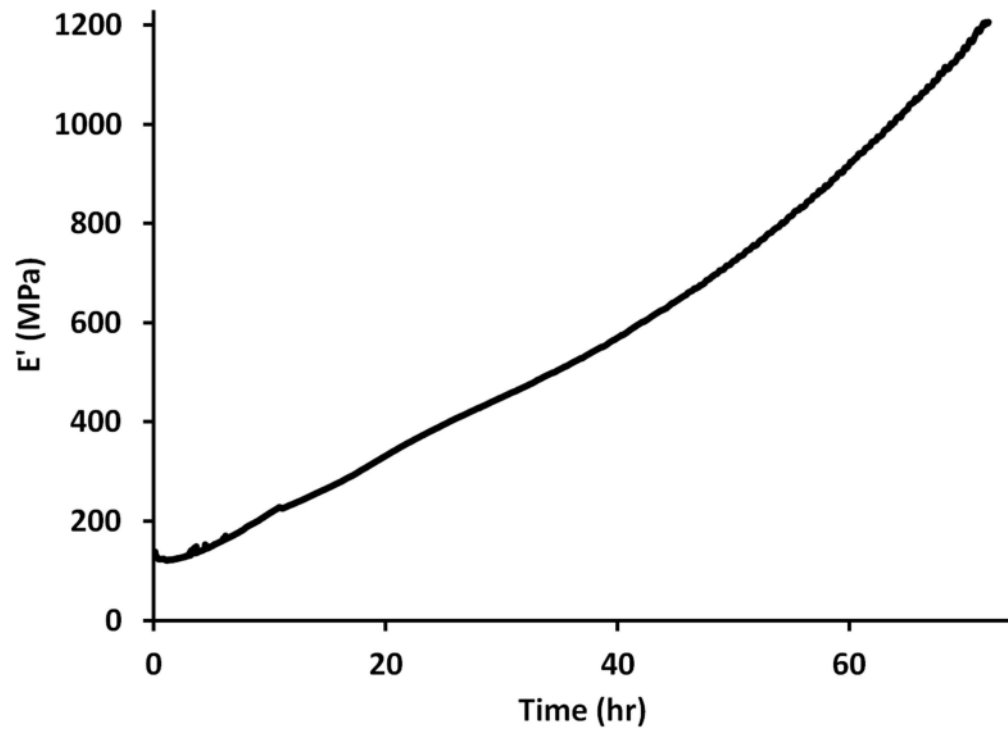


Figure 2. Dynamic mechanical analysis (DMA) of the reaction of glycerol and citric acid ([glycerol]: [citric acid] = 1) at 110°C. A sample bar (35 mm × 13 mm × 1.7 mm) was oscillated at 1 Hz in a single cantilever clamp using a 30 -m amplitude.

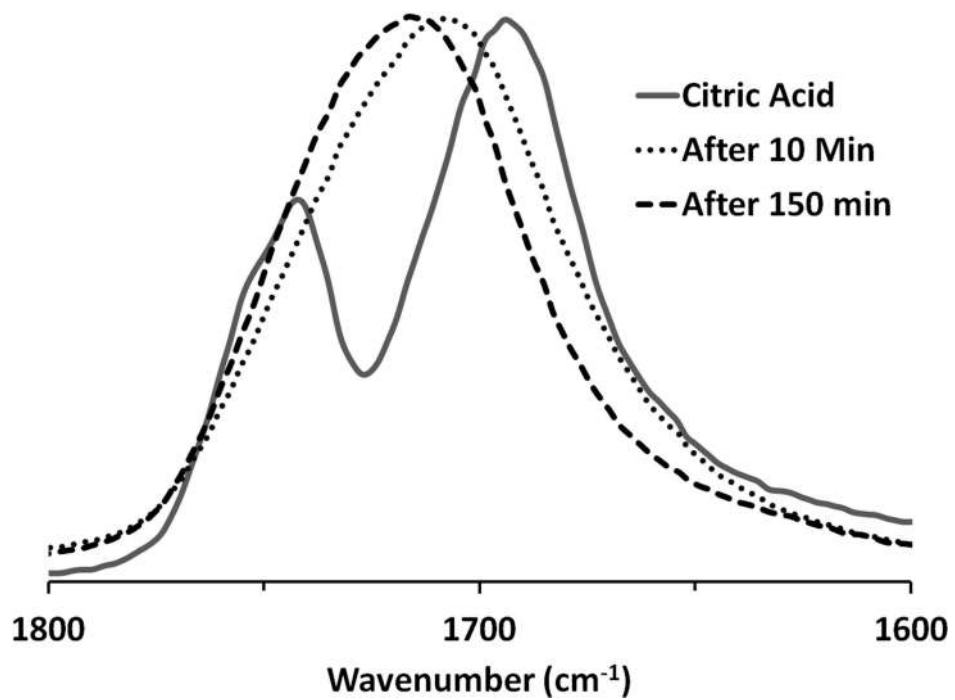


Figure 3. FTIR spectroscopy data for the reaction of glycerol and citric acid ([glycerol]:[citric acid] =1.4) at 110°C showing the carbonyl region for citric acid, product after 10 min, and product after 150 min as the ester absorbance at 1724 cm⁻¹ becomes more pronounced.

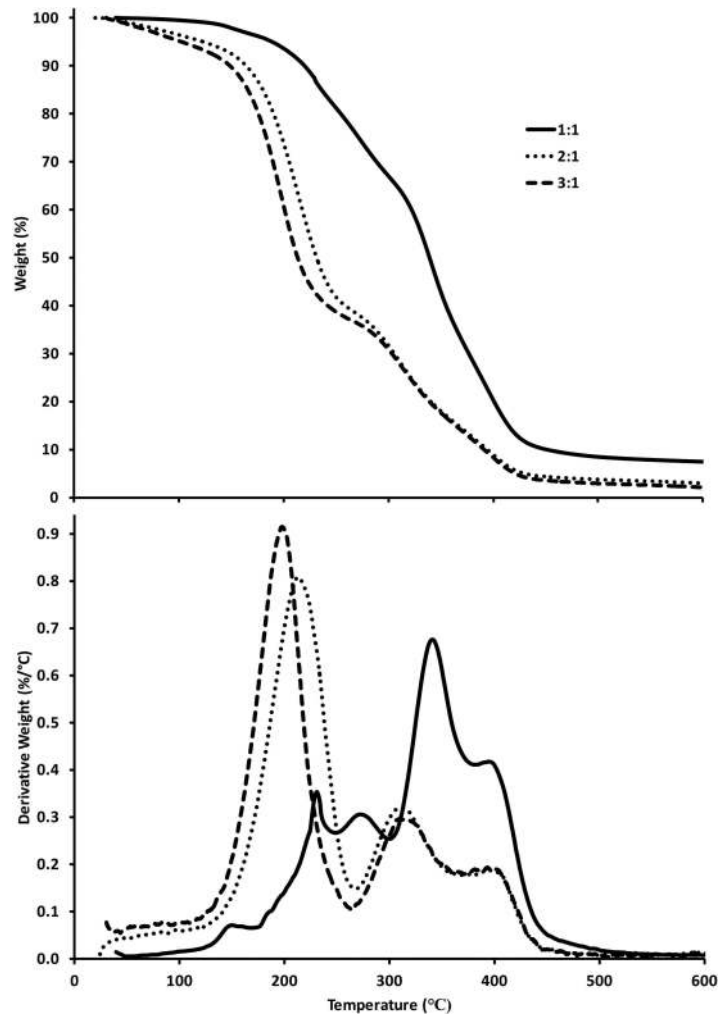


Figure 4. Overlay of TGA data (20°C/min) for reaction of glycerol and citric acid at 150°C for 1 hr using [glycerol]:[citric acid] ratios of 1:1, 2:1, and 3:1. Top: Weight percent as a function of temperature. Bottom: Derivative of weight percent as a function of temperature.

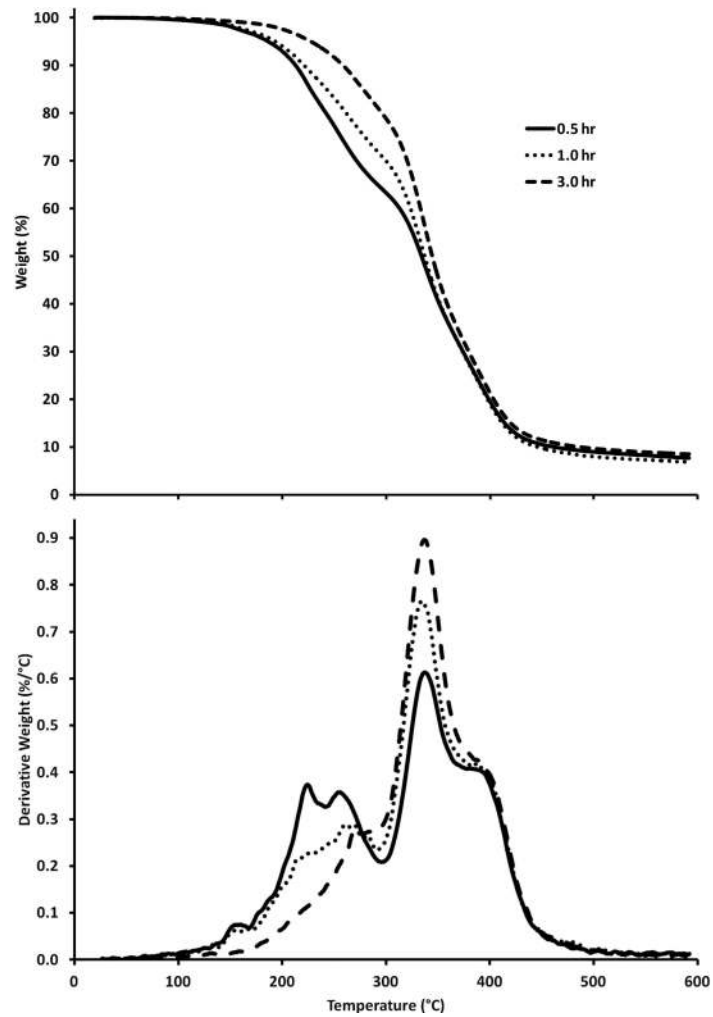


Figure 5. TGA data (20°C/min) showing the influence of time on the reaction of glycerol and citric acid of a 1:1 ratio at 150°C for 0.5 hr, 1.0 hr, and 3.0 hr. Top: Weight percent as a function of temperature. Bottom: Derivative of weight percent as a function of temperature.

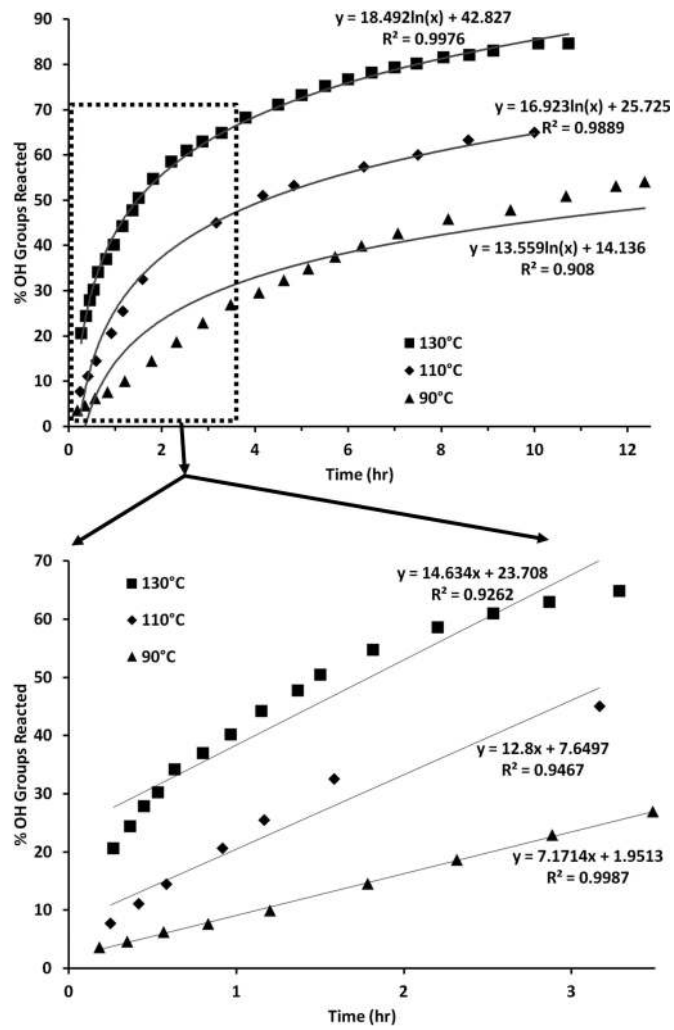


Figure 6. Kinetic data for reaction of glycerol and citric acid ([glycerol]:[citric acid] = 1) at 130°C, 110°C, and 90°C. Top: A logarithmic relationship is observed for esterification reactions up to 12.5 hrs. Polymers fabricated at 130°C show the most accurate logarithmic profile. Bottom: Linear relationships are observed for esterification reactions for the first 3.5 hrs. Polymers fabricated at 90°C have the most linear control in the first 3.5 hrs.

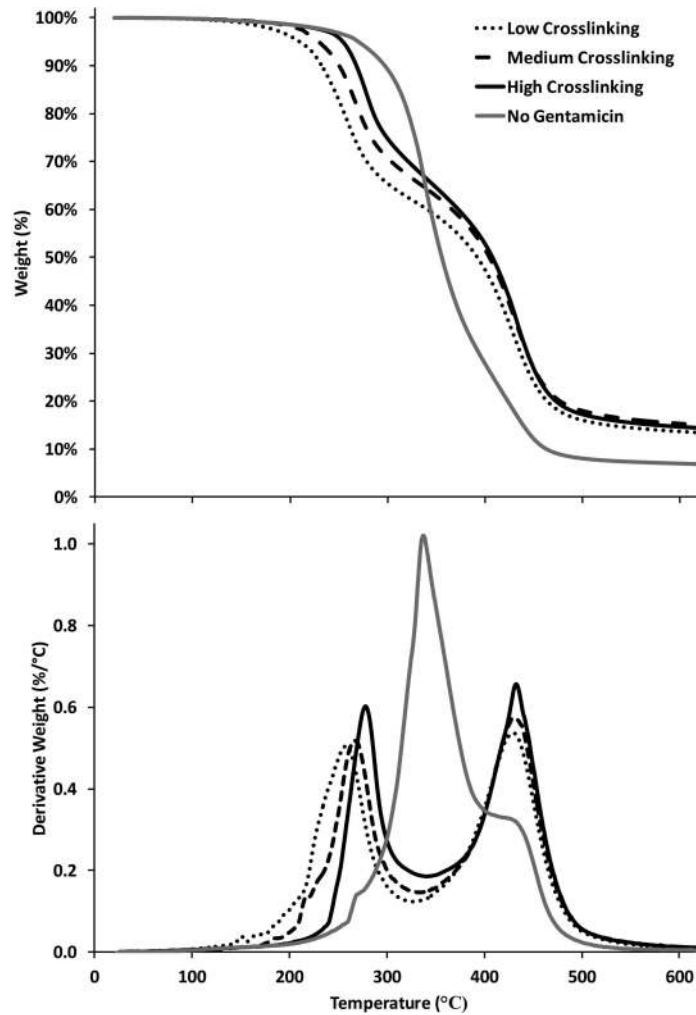


Figure 7. Comparing different amounts of polymer cross-linking within gentamicin-loaded melts. The low, medium, and high cross-linking is determined by the amount of time the polymers were reacted, 7 hr, 15 hr, and 48 hr respectively. The no gentamicin polymer was shown as a control. Top: Weight percent as a function of temperature. Bottom: Derivative of weight percent as a function of temperature.

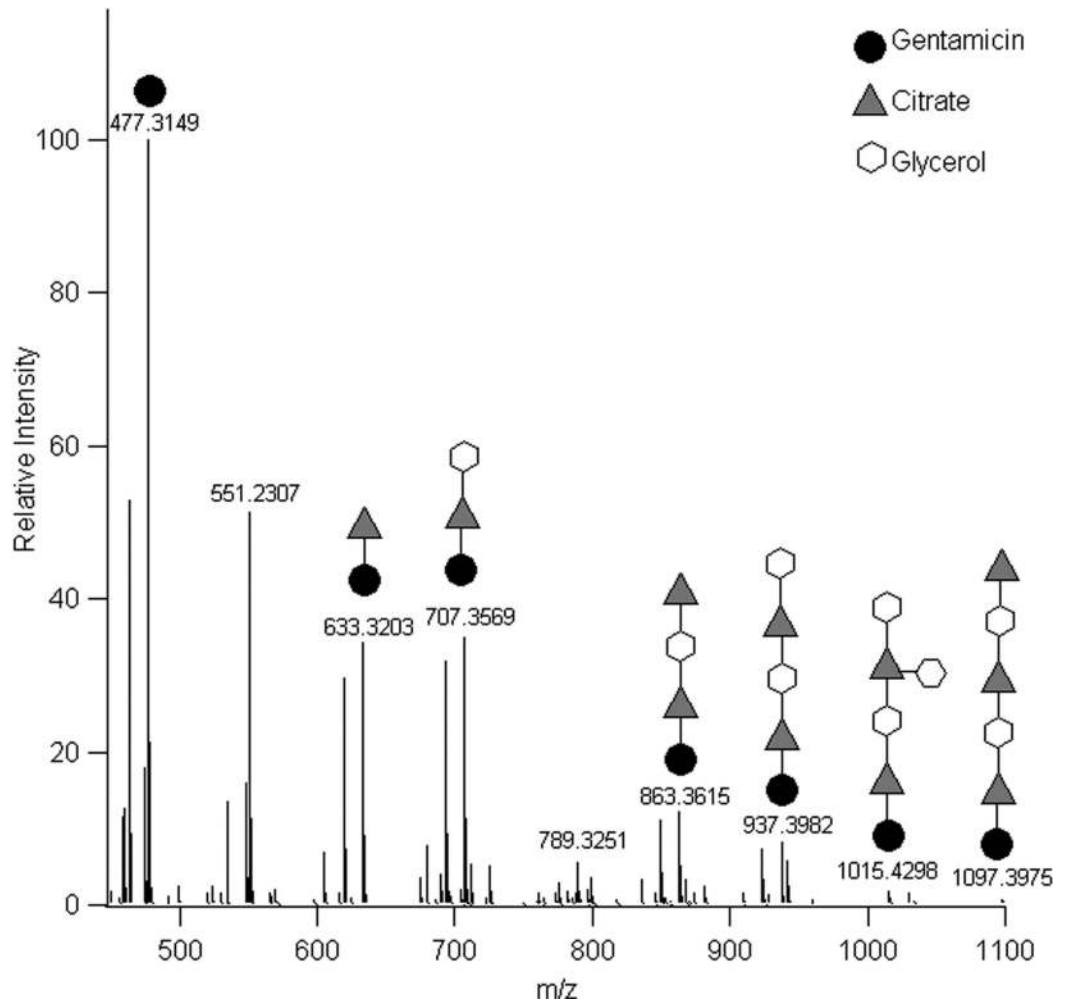


Figure 8.

Mass spectral data confirming that free gentamicin is released into aqueous environments as well as gentamicin oligomers containing citric acid and glycerol. The gentamicin (circle), citric acid (triangle), and glycerol (hexagon) conjugates illustrated in the figure do not indicate any specific orientation, and only one possibility is shown for each peak.

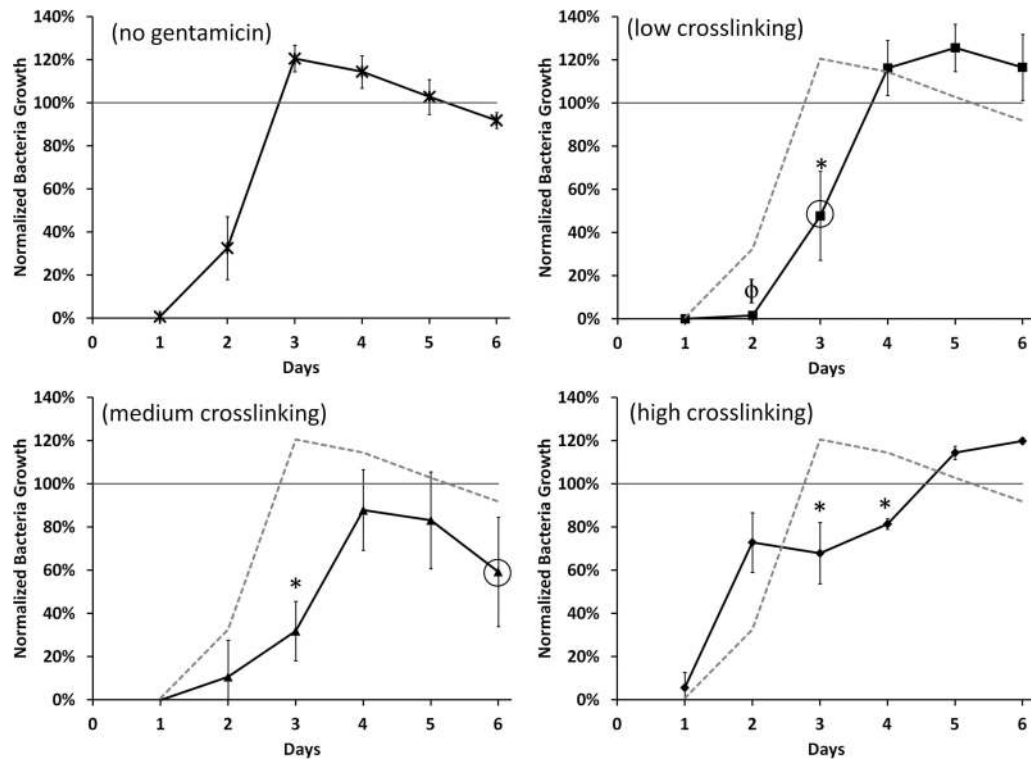


Figure 9. Percent of bacteria growth normalized to bacteria grown in soy broth with no polymer. Circles indicate when the polymer was fully degraded. No significant amount of bacteria clearing was observed after the polymers degraded. The initial bacteria clearing is associated with unbound surface citric acid release and resulting pH drop. Later clearing is associated with gentamicin release. (ϕ =p<0.05 and *=p<0.005 compared to (a) polymer with no gentamicin).

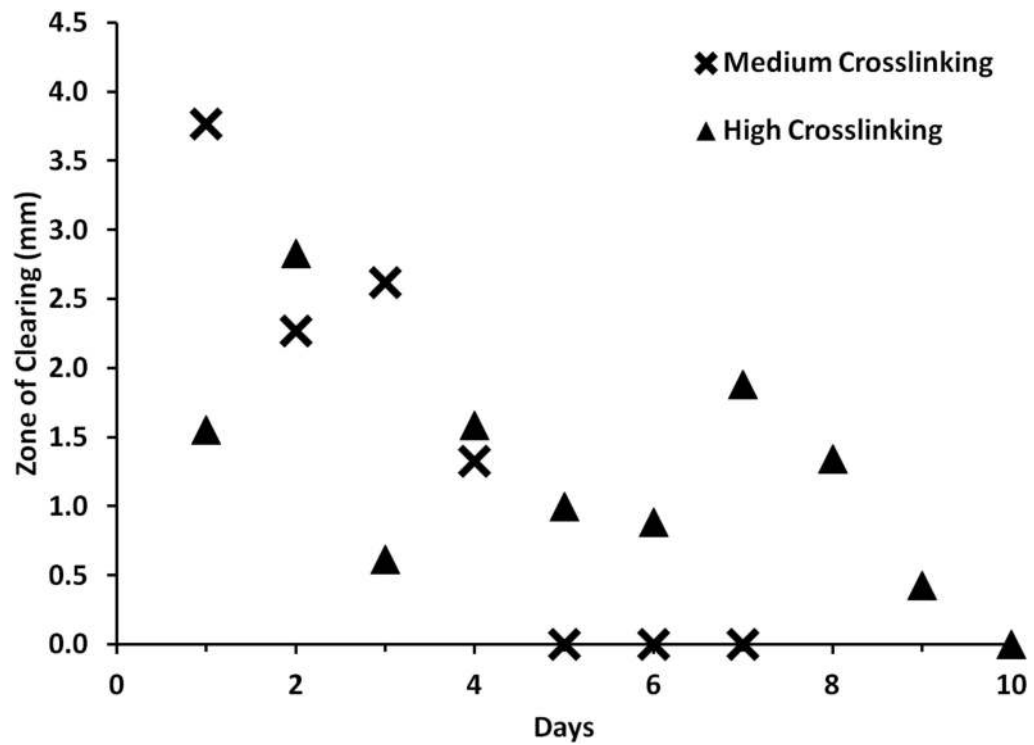
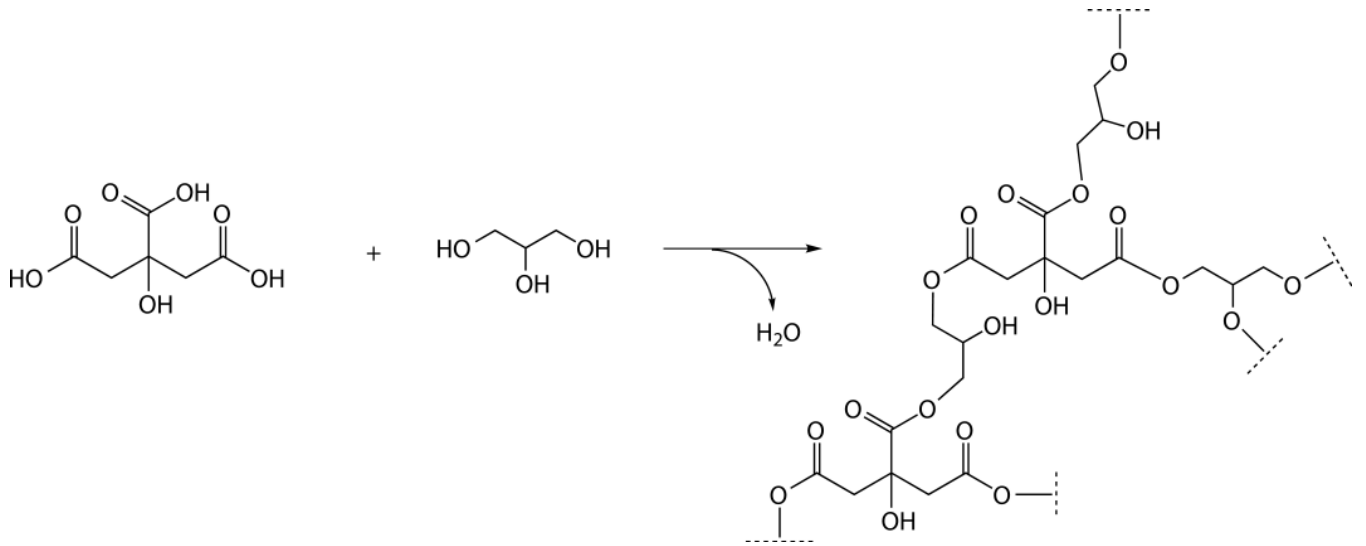


Figure 10. Zone-of-Inhibition assay results of bacteria clearing of medium and high crosslinked polymers. Inhibition zones were observed in medium and high crosslink polymers for up to 4 days and 9 days respectively. Medium crosslink polymers showed greater zones for Days 1 and 3 possibly due to the larger amount of initial gentamicin release.

**Scheme 1.**